DOI 10.15826/rjcst.2015.1.009 УДК 533

Noskov A. S.[1], *Alekhin V. N.*[2], *Khait A. V.*[3], *Anoshin N. M.*[4]
[1–4] Ural Federal University,
Yekaterinburg, Russia

E-mail: [1, 2]*referetsf@yandex.ru,* [3]*hait@mail.ru,* [4]*anoshin@e1.ru*

VISUALIZATION OF AIR FLOW IN VORTEX TUBE USING DIFFERENT TURBULENCE MODELS

Abstract. Visualization of air flow in Ranque-Hilsch vortex tube performed by numerical simulations with standard k-ε and SAS-SST turbulence models is presented in the paper. SAS-SST turbulence model predicted the existence of secondary large-scale vortex structures within the computational domain instead k-ε model showed axisymmetrical flow. Existence of large-scale secondary vortex structures is in agreement with experimental data.

Keywords: Ranque-Hilsch effect, vortex tube, CFD, turbulence modeling, visualization.

Носков А. С.[1], *Алехин В. Н.*[2], *Хаит А. В.*[3], *Аношин Н. М.*[4]
[1–4] Уральский федеральный университет,
Екатеринбург, Россия

E-mail: [1, 2]*referetsf@yandex.ru,* [3]*hait@mail.ru,* [4]*anoshin@e1.ru*

ВИЗУАЛИЗАЦИЯ ПОТОКА ВОЗДУХА В ВИХРЕВОЙ ТРУБЕ С ИСПОЛЬЗОВАНИЕМ РАЗЛИЧНЫХ МОДЕЛЕЙ ТУРБУЛЕНТНОСТИ

Аннотация. В статье представлены результаты визуализации потока воздуха в вихревой трубе Ранка-Хилша, выполненной с помощью численного моделирования. Были использованы k-ε и SAS-SST модели турбулентности. SAS-SST модель турбулентности показала наличие вторичных крупномасштабных вихревых структур в расчетном домене, в отличие от k-ε модели. Факт наличия крупномасштабных вторичных вихревых структур хорошо согласуется с экспериментальными данными.

Ключевые слова: эффект Ранка-Хилша, вихревая труба, моделирование турбулентности, визуализация

Introduction

At present time most buildings are equipped with state-of-the-art climate systems allowing maintenance of optimum values of humidity and air temperature within all rooms. In a winter season these systems carry out heating air in a building and in summertime provide its cooling. The principle of operation of such systems is generally based on thermodynamic cycles of coolants and such systems used to be called chillers. The typical coolants are Freon and ammonia which are not ecological ones. Chillers also have other essential disadvantages such as design complexity, high labour-output ratio and presence of toxic substances. Nevertheless chillers are widespread in civil engineering field despite their disadvantages.

Alternative way of cooling and heating is the use of Ranque-Hilsch vortex tubes [1, 2]. Atmosphere air is usually used in thermodynamic cycle of such devices to produce heat flow. The same air can be also used as a heat carrier. Therefore vortex tubes are often considered as ecological devices. They have very simple design and structure, low labour-output ratio and some other benefits.

In spite of the benefits, vortex tubes have low energy efficiency. The value of isentropic energy efficiency coefficient calculated by equation (1) is usually lower than 0.4. This is the reason why vortex tubes cannot be used widely.

$$\eta_S = \frac{\Delta I_X}{\Delta I_S} \qquad (1)$$

where ΔI_x — total enthalpy difference between inlet and cold flows of the vortex tube; ΔI_S — total enthalpy difference arising in the ideal isentropic gas expansion from the inlet to outlet pressure.

A schematic of vortex tube is shown in Fig. 1. Compressed gas is injected into the energy separation chamber through the nozzle inlet. As a result, vortex flow appears in that chamber. Outer part of the vortex flow has higher total temperature as compared the core flow. Finally, cold and hot flows are discharged at different sides of the vortex tube [1, 2].

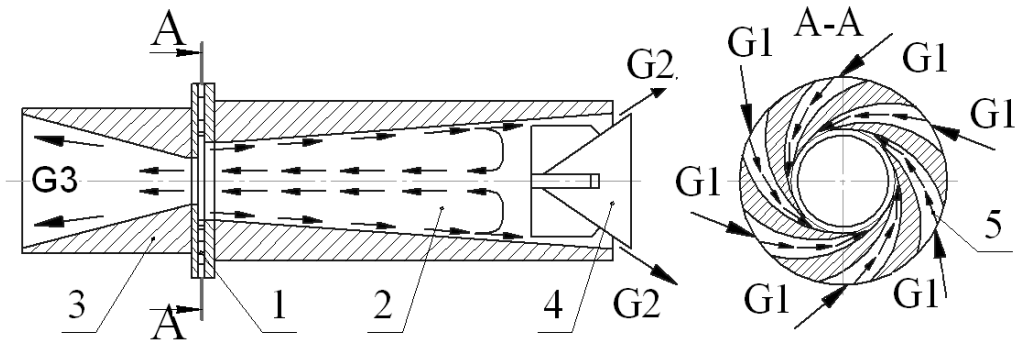

Fig. 1. Schematic of vortex tube: 1 — nozzle inlet; 2 — energy separation chamber; 3 — cold flow diffuser; 4 — hot flow throttle; 5 — nozzle duct; G1 — inlet flow; G2 — hot flow outlet; G3 — cold flow outlet

Experimental investigations, presented in the literature [1–5], highlight an ultimate complexity of the flow arising in vortex tubes. For this reason there is still no general energy separation theory which takes into account all physical processes arising in vortex tubes.

Numerical simulation is one of the ways to study the internal structure of the flow in vortex tube. Results of numerical simulation of Ranque-Hilsch effect are given in papers [6–10]. It was found out that turbulence models have significant influence on the results of simulations. For instance, Skye et al. [6] used standard k-ε turbulence model and received divergence of the ηS (Eq. 1) about 40 % with respect to experimental data. Farouk et al. [8] used LES turbulence model and found out a better coincidence with measured data.

Thus investigation of different turbulence models is important task. The present paper is aimed to investigate and visualize the air flow in Ranque-Hilsch vortex tube simulated both with standard k-ε and SAS-SST turbulence models. A detailed discussion on internal structure of the flow is given.

Numerical model

Reynolds-averaged Navier–Stokes equations were used in numerical simulations [11]:

Momentum equation

$$\rho\frac{d\mathbf{V}}{dt} = -\mathbf{grad}\left(p + \frac{2}{3}\mu_\Sigma div\mathbf{V}\right) + 2Div(\mu_\Sigma \dot{\mathbf{S}}) \quad (2)$$

where ρ — density; V — velocity; p — static pressure; $\mu\Sigma = \mu + \mu_t$; μ — molecular viscosity; μ_t — turbulence viscosity; $\dot{\mathbf{S}}$ — strain rate tensor.

Continuity equation

$$\frac{\partial\rho}{\partial t} + div(\rho\mathbf{V}) = 0 \quad (3)$$

Energy conservation equation

$$\frac{\partial}{\partial t}(\rho H) + div(\rho\mathbf{V}H) - div\left(\frac{\lambda_t}{c_p}\mathbf{grad}\,h\right) = \frac{\partial}{\partial t}p \quad (4)$$

where H — total enthalpy; h — static enthalpy; $\lambda^t/c_p = \mu_t/\mathrm{Pr}_t$; λ_t — turbulent thermal conductivity; Pr_t — turbulent Prandtl number ($\mathrm{Pr}_t = 0.8$ for air); c_p — heat capacity.

Ideal gas state equation

$$p = \rho RT \quad (5)$$

where R — gas constant

Standard k–ε and SAS-SST turbulence models [12–14] were applied. Large Eddy Simulation (LES), Detached Eddy Simulation (DES) and Reynolds Stress Models (RSM) were excluded from consideration due to limitations in computational power. ANSYS CFX was used to solve equations of the model numerically.

Computational domain of the vortex tube is depicted in Fig. 2. Main dimensions of the domain are the following: energy separation chamber diameter D = 16.8 mm; diaphragm diameter d = 9.8 mm; energy separation chamber length L = 168 mm and conical angle α = 3.5°.

The following initial conditions were used: absolute static pressure p = 105 Pa; static temperature T = 300 K; velocities $V_x = V_y = V_z = 0$; turbulence kinetic energy $k = 0$; turbulence dissipation rate ε = 0. The properties of the air were taken into consideration.

Boundary conditions:

– Vortex tube inlet (flow G_1, Fig. 1): absolute static pressure $p = 5{\cdot}105$ Pa; static temperature T = 300 K, turbulence intensity I = 5 %.

– Hot flow outlet (G_2, Fig. 1): absolute static pressure $p = 2.6{\cdot}105$ Pa. The given value of static pressure was chosen in order to obtain the cold mass flow fraction value (6) φ = 0.6.

– Cold flow outlet (G_3, Fig. 1): absolute static pressure p = 105 Pa.

– No slip and adiabatic wall boundary conditions were used at all solid walls.

– $$\varphi = \frac{G_3}{G_1} \quad (6)$$

where G_3 — cold mass flow rate; G_1 — inlet mass flow rate.

Computations were carried out in unsteady regime. Considered physical time was $t = 2{\cdot}10^{-2}$ s. Time step was

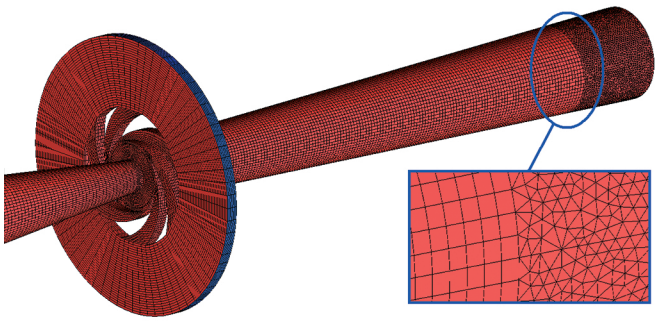

Fig. 2. Vortex tube computational domain

adaptive in the range of $\Delta t = 10^{-5}$–10^{-7} *s*. Second order scheme was used for temporal integration and high resolution scheme was used for spatial integration.

Simulation results

Distribution of hydrodynamic parameters in the longitudinal cross section of the vortex tube under consideration received with *k*-ε turbulence model is shown in Fig. 3. Analysis of the plots shows that vortex core has higher static temperature as compared to outer part of the flow. In the same time total temperature has the opposite distribution. Computational streamlines are presented in Fig. 4. The air flow is of axisymmetric and reached steady state. The flow predicted with SAS-SST turbulence model has significant differences with respect to the one predicted with *k*-ε model. The flow demonstrates unsteady

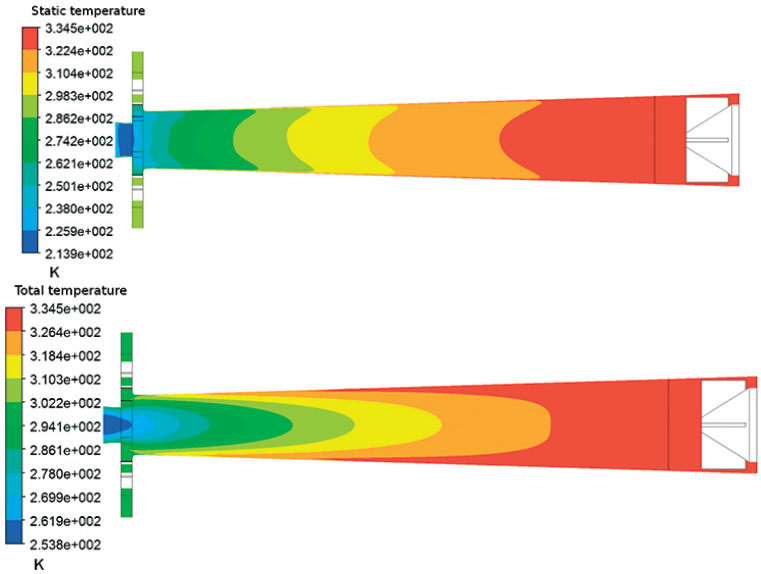

Fig. 3. Distribution of hydrodynamic parameters received with *k*-ε turbulence model

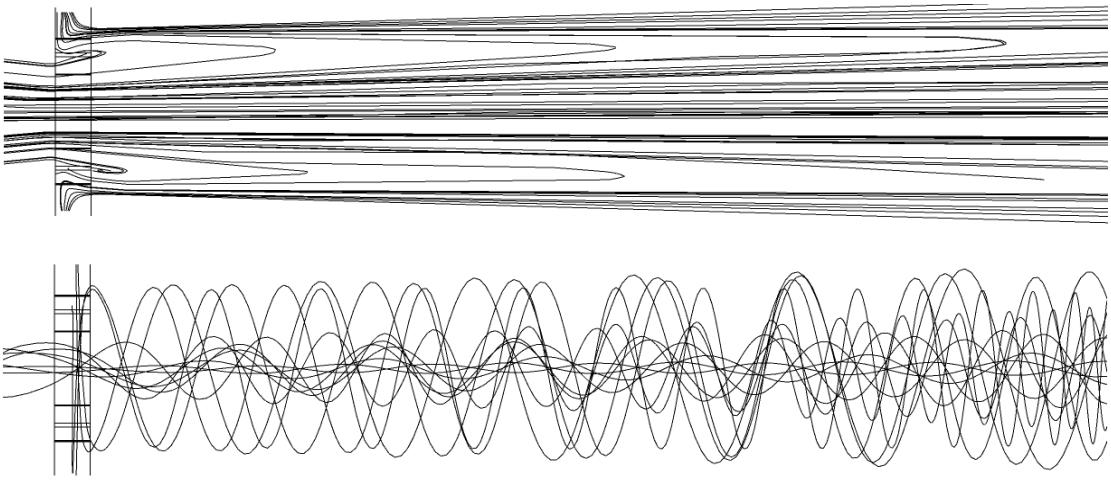

Fig. 4. Streamlines in the vortex flow predicted with k-ε turbulence model

behavior, and all hydrodynamic parameters undergo high fluctuations. Distribution of the velocity and static temperature in the longitudinal vortex tube cross section is presented in Fig. 5.

Streamlines plot is shown in Fig. 6 in order to visualize the air flow simulated with SAS-SST turbulence model. The flow is asymmetric as opposed to the one found with k-ε model. Large scale secondary vortex structures are seen in the figure. This is the main difference between the results of k-ε and SAS-SST models.

The existence of large scale vortex structures has been detected experimentally by Arbuzov et al. [15]. Experimental visualization from [15] is shown in Fig. 7.

Vortex Core Region algorithm implemented into ANSYS CFX postprocessor has been used in order to visualize secondary large-scale vortex structures predicted by SAS-SST turbulence model (Fig. 8). Qualitative agreement with experimental results (Fig. 7) is achieved. Therefore we can conclude that SAS-SST turbulence model simulates internal structure of the vortex flow in a better way with respect to standard k-ε model.

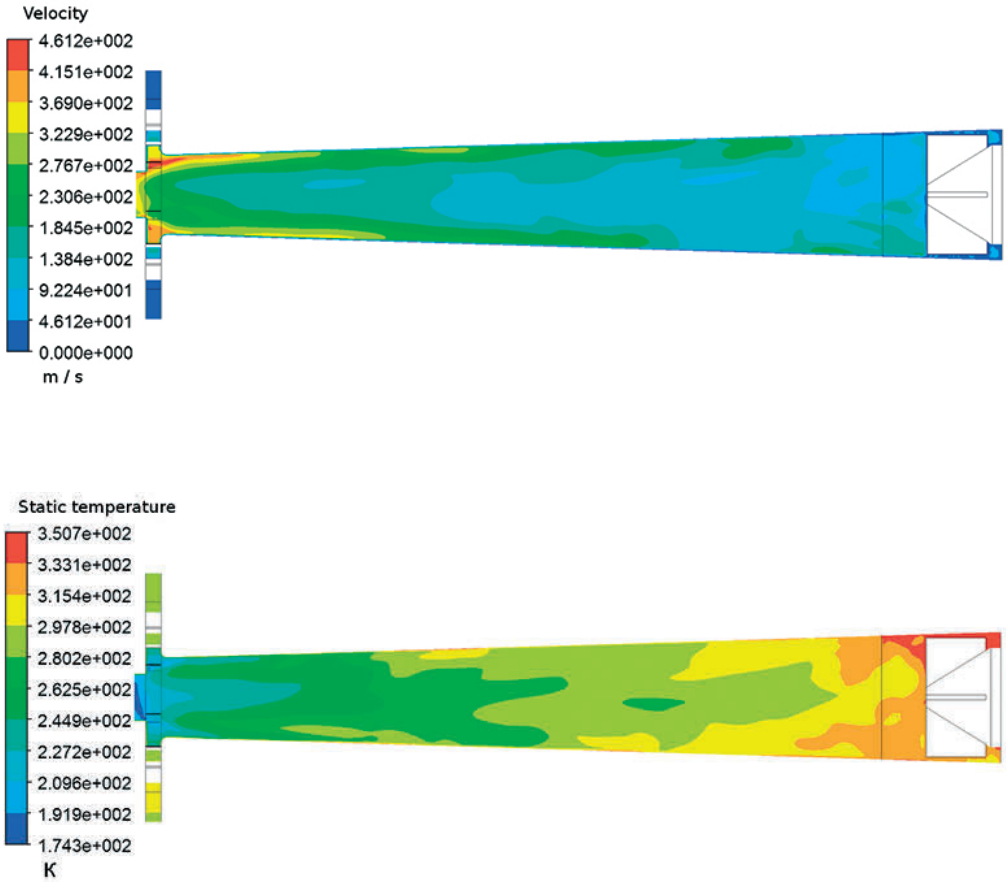

Fig. 5. Distribution of hydrodynamic parameters received with SAS-SST turbulence model

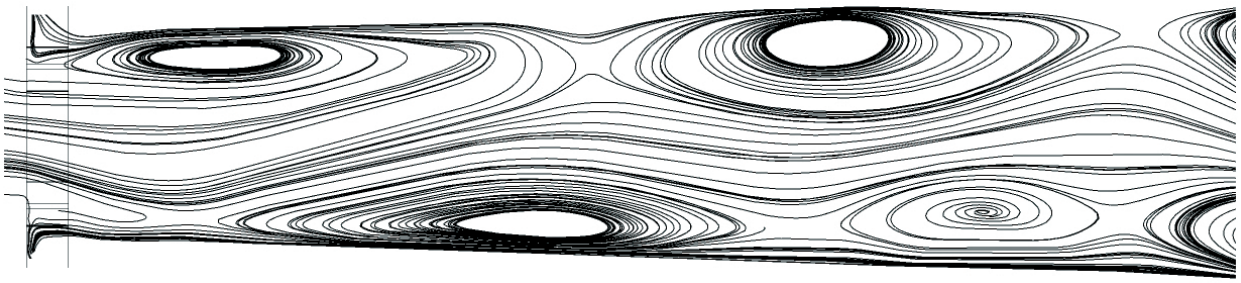

Fig. 6. Streamlines in the vortex flow predicted with SAS-SST turbulence model

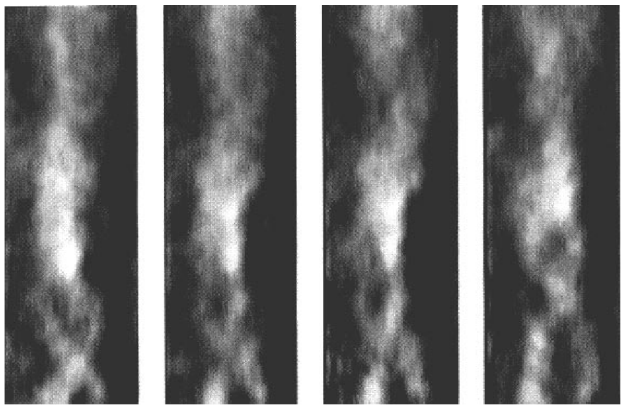

Fig. 7. Experimental visualization of secondary large-scale vortex structures [15]

Conclusion

Visualization of the air flow in Ranque-Hilsch vortex tube has been performed on the basis of numerical computations. Standard $k-\varepsilon$ and SAS-SST turbulence models were used in the simulations. SAS-SST turbulence model simulated unsteady vortex flow with high fluctuations of all hydrodynamic parameters instead k-ε model showed smooth and steady-state flow. Only SAS-SST turbulence model could predict the existence of secondary large-scale vortex structures within the computational domain. The existence of such vortex structures is confirmed by experimental results.

In conclusion, SAS-SST turbulence model is recommended for further investigation of Ranque-Hilsch energy separation phenomenon because of the better correspondence to experimental studies. Accurate numerical model of energy separation effect is a powerful instrument for improvement of the vortex tube geometry and, consequently, its efficiency.

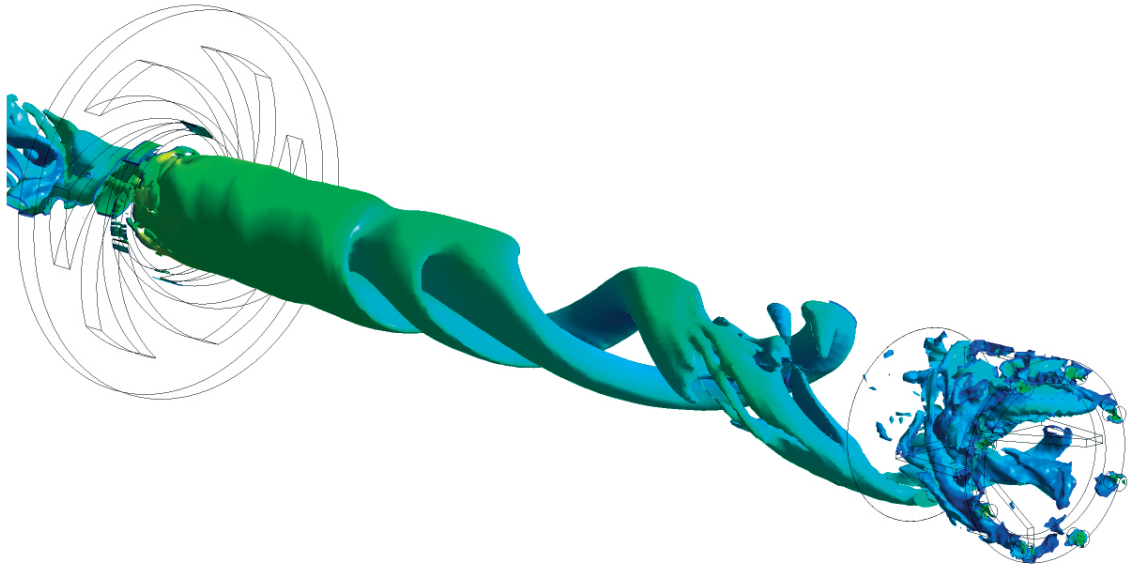

Fig. 8. Visualization of large-scale vortex structures simulated numerically with SAS-SST turbulence model

References

1. Piralishvili Sh. A., Poliaev V. M., Sergeev M. N. *Vikhrevoi effekt. Eksperiment, teoriia, tekhnicheskie resheniia* [Vortex effect. Experiment, theory, technical solutions]. Moscow, Energomash Publ., 2000. 415 p. (In Russ.).

2. Merkulov A. P. *Vikhrevoi effekt i ego primenenie v tekhnike* [Vortex effect and its application in technique]. Moscow, Mashinostroenie Publ., 1969. 184 p. (In Russ.).

3. Selek M., Tasdemir S., Dincer K. and Baskaya S. Experimental examination of the cooling performance of Ranque-Hilsch vortex tube on the cutting tool nose point of the turret lathe through infrared thermography method. *International journal of refrigeration*, 2011, vol. 34, no. 3, pp. 807–815. doi:10.1016/j.ijrefrig.2010.11.008.

4. Dincer K., Avci A., Baskaya S. and Berber A.. Experimental investigation and energy analysis of the performance of a counter flow Ranque-Hilsch vortex tube with regard to nozzle cross-section areas. *International journal of refrigeration*, 2010, no. 33, pp. 954–962

5. Chang K., Li Q. and Zhou G. Experimental investigation of vortex tube refrigerator with a divergent hot tube. *International journal of refrigeration*, 2011, no. 34, pp. 322–327.

6. Skye H. M., Nellis G. F. and Klein S. A. Comparison of CFD analysis to empirical data in a commercial vortex tube. *International journal of refrigeration*, 2006, no. 29, pp. 71–80.

7. Behera U., Paul P. J., Kasthurirengan S., Karunanithi R., Ram S. N., Dinesh K. and Jacob S. CFD analysis and experimental investigations towards optimizing the parameters of Ranque–Hilsch vortex tube. *International journal of heat and mass transfer*, 2005, no. 48, pp. 1961–1973.

8. Farouk T. and Farouk B. Large eddy simulations of the flow field and temperature separation in the Ranque–Hilsch vortex tube. *International journal of heat and mass transfer*, 2007, no. 50, pp. 4724–4735

9. Dutta T., Sinhamahapatra K. P. and Bandyopdhyay S. S. Comparison of different turbulence models in predicting the temperature separation in a Ranque–Hilsch vortex tube. *International journal of refrigeration*, 2010, no. 33, pp. 783–792.

10. Khait A., Noskov A., Alekhin V. and Lovtsov A. Mathematical simulation of Ranque-Hilsch vortex tube heat and power performances. *Proc. of 14th International conference on computing in civil and building engineering*, 2012, Moscow, pp. 160–161.

11. Loitsianskii L. G. *Mekhanika zhidkosti i gaza* [Liquid and gas mechanics]. Moscow, Drofa Publ., 2003. 840 p. (In Russ.).

12. Wilcox D. C. *Turbulence modeling for CFD*. California, DCW industries Inc., 1994. 460 p.

13. Ferziger J. H. and Peric M. *Computational methods for fluid dynamics*. Berlin et al., Springer, 2002. 423 p.

14. Menter F. R. Review of the shear-stress transport turbulence model experience from an industrial perspective. *International journal of computational fluid dynamics*, 2009, vol. 23, no. 4, pp. 305–316.

15. Arbuzov V. A., Dubnishchev Iu. N., Lebedev A. V., Pravdina M. Kh., Iavorskii N. I. Nabliudenie krupnomasshtabnykh gidrodinamicheskikh struktur v vikhrevoi trubke i effekt Ranka [Observation of large-scale hydrodynamic structures in vortex tube and Ranque effect]. *Pis'ma v ZhTF — JTF letters*, 1997, vol. 23, no. 23, pp. 84–90. (In Russ.).